Optimum Design of Symmetric Laminated Reinforced Plate Subjected to in-Plane Compressive Loading: Buckling Analysis

Article · August 2009

CITATIONS
0

READS
18

3 authors, including:

Nawras H. Mostafa
University of Babylon
21 PUBLICATIONS **24** CITATIONS
SEE PROFILE

Ahmad Saddy Mohamad
University of Babylon
12 PUBLICATIONS **4** CITATIONS
SEE PROFILE

Optimum Design of Symmetric Laminated Reinforced Plate Subjected to in-Plane Compressive Loading: Buckling Analysis

3 authors, including:

Nawras H. Mostafa
University of Babylon
17 PUBLICATIONS **18** CITATIONS

SEE PROFILE

Optimum Design of Symmetric Laminated Reinforced Plate Subjected to in-Plane Compressive Loading: Buckling Analysis

By

N. H. Mostafa, S. O. Waheed, and A. Saady

التصميم المثالي لصفيحة مقواة ذات تصفيح متماثل معرضة لحمل ضاغط ضمن المستوي: تحليل الانبعاج

نورس حيدر ، سلوان عبيد ، احمد سعدي

الخلاصة

الهدف من البحث الحالي هو دراسةحمل الانبعاج للصفائح المقواة بالألياف . إن حمل الانبعاج لتلك الصفائح يعتمد على مجموعة من المتغيرات و المتضمنة نسبة الواجهة، سُمك الصفيحة،اتجاه ألياف الصفائح الرقيقة و المكونة للصفيحة الكلية و تأثير الظروف الحدودية. هذه المتغيرات تم ربطها مع حمل الانبعاج و ذلك بتحليل عدد من الصفائح باستخدام برنامج العناصر المحددة ANSYS . من خلال البحث وجد إن أفضل ترتيب للألياف لصفيحة مقواة بالألياف ذات إسناد بسيط لجميع الحافاة هو بزاوية 45±و لجميع الاسماك ذات نسب الواجهة 1و 2 ، و تتغير هذه الحالة عند تغيير الظروف الحدودية. ففي حالة الحدود بسيط–بسيط–مثبت–مثبت كان الترتيب 30-/30+ هو الترتيب المثالي في مقاومة الانبعاج و لجميع نسب الواجهة، بينما في حالة الحدود حرة– مثبت–مثبت–مثبت كان الترتيب 15-/15+ هو الأفضل. و لجميع الحالات المذكورة أعلاه، يزداد حمل الانبعاج مع زيادة نسبة الواجهة وبالتأكيد مع زيادة سُمك الصفيحة.

Abstract:

The objective of the current research is to investigate the critical buckling load of fiber reinforced (FR) plate. The buckling load of an FR plate depends on a variety of variables, including aspect ratio, thickness of the laminate, fiber orientation of the laminae that make up the laminate, and the boundary conditions. These variables were related to the buckling load of laminated plates by analyzing a number of laminated plates using the commercially available ANSYS finite element software. Among other things, it was found that for the analyzed FR laminated plates simply supported on all edges, the optimal fiber orientation of the mat layers was ± 45 degrees for all thicknesses with aspect ratios of 1.0 and 2.0 , but that was not the case for the other boundary conditions considered. In the case of simple-simple-fixed-fixed, the +30/-30 orientation produce the highest buckling load for all aspect ratios cases considered; while for free-fixed-fixed-fixed the +15/-15 did in the majority of the cases. For all cases of the boundary conditions, critical buckling loads increase with increasing aspect ratio and of course with increasing plate thickness.

Keywords: buckling, fiiber reinforced, symmetric laminate plate, ANSYS.

1. Introduction

Over the last few decades, the critical buckling load of rectangular plates has been very extensively studied for a wide range of loading cases and boundary conditions (Huyton and York 2001). By contrast, far fewer studies have considered the buckling behavior of fiber reinforced laminated plate

structures, despite the practical importance of laminated plates in aircraft wing and fuselage panels. Fiber reinforced has been used for many years in the aerospace and automotive industries for their advantages such as lightweight, corrosion resistance, low thermal and electrical conductivity, high strength to weight and stiffness to weight ratios, and the ability to vary the properties over a wide range of values. Although various materials can be used as fiber reinforcement, the most common used are glass, carbon, and organic fibers (Barbero, 1999). The type of fiber used depends on the application, the properties desired, and the cost. Glass is the most common type of fiber used because of its low cost. The laminated plates are subjected to any combination of in plane, out of plane and shear loads during application. Due to the geometry of these structures, buckling is one of the most important failure criteria.

Many researchers were studied the buckling of rectangular plates. Exact and approximate solutions have been derived. There are many exact solutions for linear elastic isotropic thin plates; many treated by Timoshenko (1961). The mechanical properties of composite materials are often approximated as orthotropic. Buckling of orthotropic plates has been the subject of many investigations during the past. According to Vakiener, Zureick, and Will (1991), the first treatment of the stability of an orthotropic plate with one free edge was done by Trayer and March in 1931. An energy solution was presented for the stability of an elastically restrained flange with orthotropic properties. Ashton and Waddoups (1969) determined critical buckling loads for the general case of anisotropic plates. Using an approximate Rayleigh-Ritz solution, they presented solution techniques for the buckling load of laminated rectangular anisotropic plates. Ashton and Whitney (1970) formulated approximate buckling load equations for laminated plates. They treated the specially orthotropic laminate case as equivalent to homogeneous orthotropic plates. Khdeir (1989) investigated the stability of antisymmetric angle-ply laminated plates. Khdeir used a generalized Levy type solution to determine the compressive buckling loads of rectangular shaped plates. He showed the influence of the number of layers, lamina orientation, and the type of boundary conditions on buckling response characteristics of composite plates. Pandey and Sherbourne (1991) used energy methods to present a general formulation for the buckling of rectangular anisotropic symmetric angle-ply composite laminates under linearly varying, uniaxial compressive force. The plates were subjected to four different combinations of simple and fixed boundary conditions. The results showed that $\theta = 45$ degrees is the optimal fiber angle for laminates with simply supported loaded edges under a wide range of stress gradients. Chen (1994) used energy methods to determine the buckling mode change of antisymmetric angle-ply laminates. Chen evaluated numerically the effects of lamination angle, length-to-thickness ratio, aspect ratio, modulii ratio and boundary conditions on the change of buckling modes. Bao, Jiang and Roberts (1997) used finite element solutions to critically review this exact solution for buckling of rectangular orthotropic plates. They found that for plates with all edges simply supported the solution is accurate. Veres and Kollar (2001) presented closed form approximate formulas for the calculation of rectangular orthotropic plates with clamped and/or simply supported edges. They used these formulas and finite element to compare to the exact solutions obtained by Whitney and the formulas were found to over estimate the buckling load by less than 8%.

2. Macromechanics of a Lamina

The goal of macromechanics of a lamina is to determine the stress-strain behavior of an individual lamina. Since a laminate is made up of laminae with various fiber orientations, the stress-strain relationships for a lamina is first expressed in terms of the lamina coordinate system and then transformed to the global coordinate system of the laminate. This is necessary in order to determine the stiffness of a laminate in terms of the global coordinate system.

2.1 Stress-Strain Relationship in a Lamina

Using contracted notation, the generalized Hooke's law relating stresses to strains is

$$\{\sigma_i\} = [C_{ij}]\{\varepsilon_j\} \tag{1}$$

where, σ_i are the stress components, C_{ij} is the 6 * 6 constitutive matrix, and ε_j are the strain components. The stiffness matrix has 36 constants, but by using energy methods it can be shown that the stiffness matrix is symmetric ($C_{ij}=C_{ji}$) and therefore only 21 of the constants are independent (Jones, 1999). The relationship in Eq.(1) characterizes an anisotropic material, which has no planes of symmetry for the material properties. For a lamina, which is considered to be orthotropic, the stiffness matrix has only nine independent constants.

2.1.1 Lamina Coordinate System.

Assuming a state of plane stress in the 1-2 material plane gives:

$$\sigma_{33} = \sigma_{23} = \sigma_{31} = 0 \tag{2}$$

which reduces Hooke's law to:

$$\begin{Bmatrix} \sigma_1 \\ \sigma_2 \\ \tau_{12} \end{Bmatrix} = \begin{bmatrix} Q_{11} & Q_{12} & 0 \\ Q_{12} & Q_{22} & 0 \\ 0 & 0 & Q_{66} \end{bmatrix} \begin{Bmatrix} \varepsilon_1 \\ \varepsilon_2 \\ \gamma_{12} \end{Bmatrix} \tag{3}$$

where [Q] is the reduced stiffness matrix. The components of the reduced stiffness matrix are defined in terms of the in-plane mechanical properties of the lamina and are

$$\begin{aligned} Q_{11} &= \frac{E_1}{1-\upsilon_{12}\upsilon_{21}} \\ Q_{12} &= \frac{\upsilon_{12}E_2}{1-\upsilon_{12}\upsilon_{21}} = \frac{\upsilon_{21}E_1}{1-\upsilon_{12}\upsilon_{21}} \\ Q_{22} &= \frac{E_2}{1-\upsilon_{12}\upsilon_{21}} \\ Q_{66} &= G_{12} \end{aligned} \tag{4}$$

2.1.2 Global Coordinate System.

The response of a laminate to loading in the global coordinate system is found using the stress-strain relationships, determined in terms of the global coordinate system, of each lamina. Generally, Eq. 3 must be transformed to reflect rotated fiber orientation angles. The following relationship reflects this transformation [Brian,1998]:

$$\begin{Bmatrix} \sigma_x \\ \sigma_y \\ \tau_{xy} \end{Bmatrix} = \begin{bmatrix} \overline{Q}_{11} & \overline{Q}_{12} & \overline{Q}_{16} \\ \overline{Q}_{12} & \overline{Q}_{22} & \overline{Q}_{26} \\ \overline{Q}_{16} & \overline{Q}_{26} & \overline{Q}_{66} \end{bmatrix} \begin{Bmatrix} \varepsilon_x \\ \varepsilon_y \\ \gamma_{xy} \end{Bmatrix} \tag{5}$$

where [$\overline{Q}$] is the transformed reduced stiffness matrix, which is found using the relation

$$\left[\overline{Q}\right] = [T]^{-1}[Q][T]^{-T} \tag{6}$$

where the superscript T denotes the matrix transpose and [T] is the transformation matrix, which is

$$[T]=\begin{bmatrix} m^2 & n^2 & 2mn \\ n^2 & m^2 & -2mn \\ -mn & mn & m^2-n^2 \end{bmatrix} \tag{7}$$

where $m = \cos\theta$, $n = \sin\theta$ and θ is the angle between the lamina's coordinate system and the global coordinate system as shown in Fig. 1.

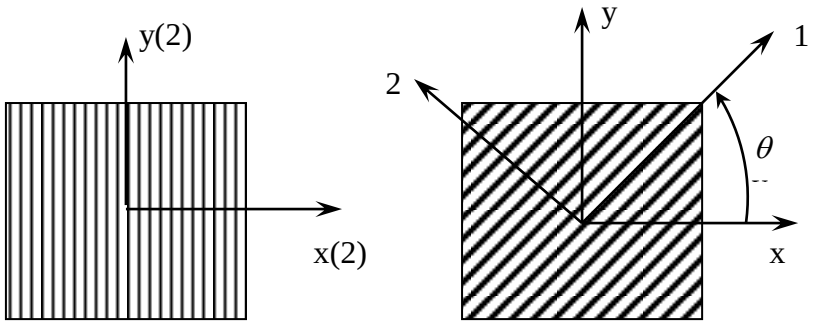

Figure 1: Lamina On- and Off-axis Configurations (Staab, 1999)

Using Eq. (6) and Eq. (7), the components of the transformed reduced stiffness matrix are

$$\begin{aligned}
\overline{Q}_{11} &= Q_{11}m^4 + 2(Q_{12}+2Q_{66})m^2n^2 + Q_{22}n^4 \\
\overline{Q}_{12} &= (Q_{11}+Q_{22}-4Q_{66})m^2n^2 + Q_{12}(m^4+n^4) \\
\overline{Q}_{22} &= Q_{11}n^4 + 2(Q_{12}+2Q_{66})m^2n^2 + Q_{22}m^4 \\
\overline{Q}_{16} &= (Q_{11}-Q_{12}-2Q_{66})m^3n + (Q_{12}-Q_{22}+2Q_{66})mn^3 \\
\overline{Q}_{26} &= (Q_{11}-Q_{12}-2Q_{66})mn^3 + (Q_{12}-Q_{22}+2Q_{66})m^3n \\
\overline{Q}_{66} &= (Q_{11}+Q_{22}-2Q_{12}-2Q_{66})m^2n^2 + Q_{66}(m^4+n^4)
\end{aligned} \tag{8}$$

Note that the transformed reduced stiffness matrix, [$\overline{Q}$], has terms in all positions in the matrix as opposed to the presence of zeros in the reduced stiffness matrix, [Q]. Therefore, in terms of the global coordinate system, a generally orthotropic lamina appears to be anisotropic, since shear-extension coupling exists (Jones, 1999).

2.2 Variation of Strain and Stress in a Laminate

The strain of any point in a laminate that has undergone deformation can be determined by considering the geometry of the undeformed and deformed cross section shown in Fig. 2. Point B in this figure is located at the mid-plane and in going from the undeformed to the deformed shape Point B undergoes a displacement in the x-direction of u_o. (Note that the symbol 'nought' (o) designates mid-plane values of a variable) Since, due to Kirchhoff's hypothesis, line ABCD remains straight under deformation of the laminate, the displacement of arbitrary point C is

$$u_c = u_o - z_c\beta \tag{9}$$

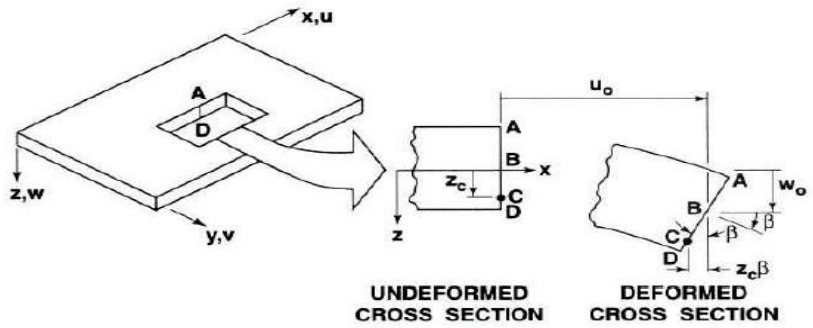

Figure 2: Geometry of Deformation (Jones, 1999)

Based on Kirchhoff's hypothesis, under deformation, line ABCD remains perpendicular to the mid-plane; therefore, β is the slope of the laminate mid-plane in the x-direction, that is,

$$\beta = \frac{\partial w_o}{\partial x} \tag{10}$$

The displacement, *u*, at any point *z* through the thickness of the laminate is

$$u = u_o - z\frac{\partial w_o}{\partial x} \tag{11}$$

Similarly, the displacement, *v*, in the y-direction is

$$v = v_o - z\frac{\partial w_o}{\partial y} \tag{12}$$

According to Kirchhoff's hypothesis $\varepsilon_z = \gamma_{xz} = \gamma_{yz} = 0$, therefore the remaining non-zero laminate strains are ε_x, ε_y, and γ_{xy}. Combining these relationships with Eq. 5 gives the following expression for the k^{th} layer:

$$\begin{Bmatrix}\sigma_x\\ \sigma_y\\ \tau_{xy}\end{Bmatrix}_k = \begin{bmatrix}\overline{Q}_{11} & \overline{Q}_{12} & \overline{Q}_{16}\\ \overline{Q}_{12} & \overline{Q}_{22} & \overline{Q}_{26}\\ \overline{Q}_{16} & \overline{Q}_{26} & \overline{Q}_{66}\end{bmatrix}_k \left[\begin{Bmatrix}\varepsilon_x^{\,o}\\ \varepsilon_y^{\,o}\\ \gamma_{xy}^{\,o}\end{Bmatrix} + z\begin{Bmatrix}\kappa_x\\ \kappa_y\\ \kappa_{xy}\end{Bmatrix}\right] \tag{13}$$

Even though the strain variation is linear through the thickness of a laminate, the stress variation is not necessarily linear through the thickness of a laminate because the transformed reduced stiffness matrix, [$\overline{Q}$], can be different for each lamina in a laminate.

By integrating through the thickness of the laminate, the net force resultants and moment resultants can be calculated.

$$\begin{Bmatrix}N_x\\ N_y\\ N_{xy}\end{Bmatrix} = \int_{-t/2}^{t/2}\begin{Bmatrix}\sigma_x\\ \sigma_y\\ \tau_{xy}\end{Bmatrix}dz = \sum_{k=1}^{N}\int_{z_{k-1}}^{z_k}\begin{Bmatrix}\sigma_x\\ \sigma_y\\ \tau_{xy}\end{Bmatrix}_k dz \tag{14}$$

and

$$\begin{Bmatrix}M_x\\ M_y\\ M_{xy}\end{Bmatrix} = \int_{-t/2}^{t/2}\begin{Bmatrix}\sigma_x\\ \sigma_y\\ \tau_{xy}\end{Bmatrix}zdz = \sum_{k=1}^{N}\int_{z_{k-1}}^{z_k}\begin{Bmatrix}\sigma_x\\ \sigma_y\\ \tau_{xy}\end{Bmatrix}_k zdz \tag{15}$$

where z_k and z_{k-1} are defined in the geometry of an *N*- layered laminate, which is depicted in Fig. 3.

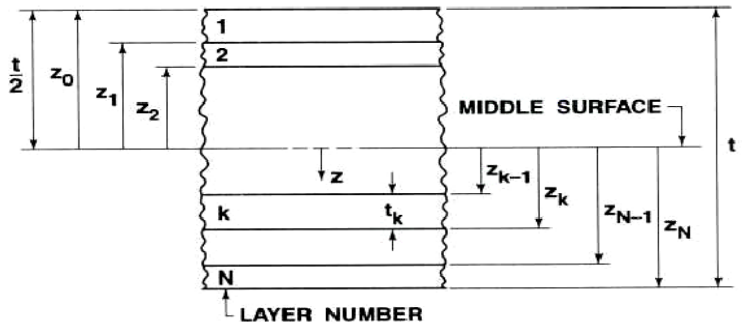

Figure 3: Geometry of an N-Layered Laminate (Jones, 1999)

Combining these relationships with Eq. 13 gives:

$$\begin{Bmatrix} N_x \\ N_y \\ N_{xy} \end{Bmatrix} = \begin{bmatrix} A_{11} & A_{12} & A_{16} \\ A_{12} & A_{22} & A_{26} \\ A_{16} & A_{26} & A_{66} \end{bmatrix} \begin{Bmatrix} \varepsilon_x^{\,o} \\ \varepsilon_y^{\,o} \\ \gamma_{xy}^{\,o} \end{Bmatrix} + \begin{bmatrix} B_{11} & B_{12} & B_{16} \\ B_{12} & B_{22} & B_{26} \\ B_{16} & B_{26} & B_{66} \end{bmatrix} \begin{Bmatrix} \kappa_x \\ \kappa_y \\ \kappa_{xy} \end{Bmatrix} \tag{16}$$

$$\begin{Bmatrix} M_x \\ M_y \\ M_{xy} \end{Bmatrix} = \begin{bmatrix} B_{11} & B_{12} & B_{16} \\ B_{12} & B_{22} & B_{26} \\ B_{16} & B_{26} & B_{66} \end{bmatrix} \begin{Bmatrix} \varepsilon_x^{\,o} \\ \varepsilon_y^{\,o} \\ \gamma_{xy}^{\,o} \end{Bmatrix} + \begin{bmatrix} D_{11} & D_{12} & D_{16} \\ D_{12} & D_{22} & D_{26} \\ D_{16} & D_{26} & D_{66} \end{bmatrix} \begin{Bmatrix} \kappa_x \\ \kappa_y \\ \kappa_{xy} \end{Bmatrix} \tag{17}$$

where

$$\begin{aligned} A_{ij} &= \sum_{k=1}^{N} (\overline{Q}_{ij})_k (z_k - z_{k-1}) \\ B_{ij} &= \frac{1}{2} \sum_{k=1}^{N} (\overline{Q}_{ij})_k (z_k^2 - z_{k-1}^2) \\ D_{ij} &= \frac{1}{3} \sum_{k=1}^{N} (\overline{Q}_{ij})_k (z_k^3 - z_{k-1}^3) \end{aligned} \tag{18}$$

The extensional stiffness matrix is [*A*], the bending-extension coupling stiffness matrix is [*B*], and the bending stiffness matrix is [*D*]. The presence of matrix [*B*] implies that there is a coupling between bending and extension, therefore if a laminate has B_{ij} terms, pulling on the laminate will cause bending and/or twisting of the laminate. The terms A_{16} and A_{26} represent shear-extension coupling, which means coupling exist between shear stress and normal strains and between normal stresses and shear strain, in a laminate. The terms D_{16} and D_{26} represent bending-twisting coupling in a laminate. The [*A*], [*B*], and [*D*] matrices are very useful in understanding the behavior of a laminate under given loading conditions and are used frequently in the analysis of composites.

3. Laminate Plate Buckling

This section deals with the analytical determination of the critical buckling load of various types of plates. Buckling of a plate occurs when the in-plane compressive load gets large enough to cause a sudden lateral deflection of the plate. Initially a plate under compressive load undergoes only in-plane deformations, but as this compressive load gets large, the plate reaches its critical buckling load, the load at which a sudden lateral deflection of the plate takes place.

The critical buckling load of a plate will be determined in two ways: **(1)** using previously derived equations, and **(2)** using the finite element program ANSYS, version 9. In using ANSYS to determine buckling loads for laminated plates, the effect of layer orientation, boundary conditions,

plate aspect ratio, and laminate thickness on the critical buckling load of laminated plates is taken into consideration.

A general plate subjected to an in-plane load is shown in Fig. 4, where N_x is critical buckling load. The aspect ratio, which is an important quantity in plate buckling, is defined as length 'a' divided by width 'b'. The boundary condition notation used (e.g., free-fixed-fixed-fixed) refers to the boundary conditions along edge (x = 0)-(y = 0)-(x = a)-(y = b).

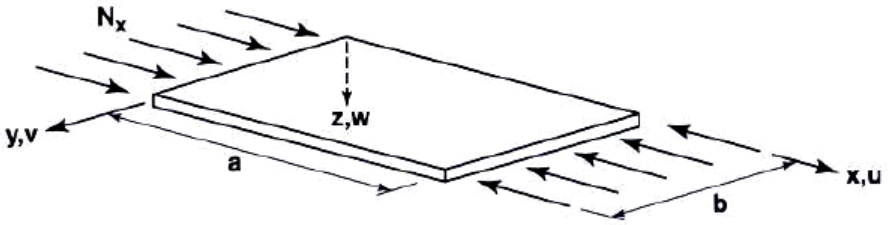

Figure 4: Plate Subjected to Uniform Uniaxial In-Plane Compression (Jones, 1999)

3.1 Analytical Critical Buckling Load of Laminated Plates Using Previous Derived Equations

Buckling of FR laminated plates is a complicated topic, and buckling solutions for only a few laminate cases have been published. The solution that will be presented is for a symmetric, specially orthotropic laminated plate simply supported on all edges. A specially orthotropic laminate has no shear-extension coupling ($A_{16} = A_{26} = 0$), no bend-twist coupling ($D_{16} = D_{26} = 0$), and no bending-extension coupling ($[B] = 0$). The critical buckling load for a symmetric, specially orthotropic laminated plate simply supported on all edges is, (Jones, 1999)

$$(N_x)_{cr} = \frac{\pi^2 D_{22}}{b}\left[\mathrm{m}^2 \frac{D_{11}}{D_{22}}\left(\frac{b}{a}\right)^2 + 2\left(\frac{D_{12}+2D_{66}}{D_{22}}\right) + \frac{1}{\mathrm{m}^2}\left(\frac{a}{b}\right)^2\right] \tag{19}$$

Where m is the number of half-waves of the buckled shape in the x-direction

As can be seen by Eq. 19, the buckling load is dependent on the components of the bending stiffness matrix. Eq. 19 will produce erroneous results for laminates with nonzero values of D_{16} and D_{26}. For laminates that have values for D_{16} and D_{26} (bend-twist coupling exists) the principal influence is to lower the buckling load obtained with Eq. 19. Therefore, the specially orthotropic solution is considered an unconservative approximation to the general class of laminates that usually have bend-twist coupling. The approximation of a general laminate by a specially orthotropic laminate can result in errors as big as a factor of 3 (Jones, 1999). A more accurate solution for the buckling load of general laminated plates (laminates having no zero terms for all components of the bending stiffness matrix) has been done, but the solution procedure is complicated. Eq. 19 is considered suitable for this work and is compared to ANSYS buckling load results for laminates simply supported on all edges.

3.2 Critical Buckling Load of Laminated Plates Using ANSYS

Critical buckling loads of various plates were found using the commercially available finite element software, ANSYS, version 9. Using ANSYS, an eigenvalue buckling analysis was done to determine the critical buckling load. Eigenvalue buckling analysis predicts the bifurcation point (the critical buckling load) of an ideal linear elastic structure. It should be noted that using this approach will often yield unconservative results when compared to "real-world" structures which rarely ever reach their theoretical buckling load due to imperfections, non-linearties, etc. For the purpose of this

research, eigenvalue analysis is an appropriate tool to use since the concern is to see the general effects, on the critical buckling load, of changing the make up, physical dimensions, and/or properties laminate plates.

ANSYS was used to analyze the critical buckling load of various laminated plates in order to see how changes in the laminated plate would affect the buckling load. The changes to the laminated plate were based on four variables: boundary condition, thickness, aspect ratio and orientation of the stitched mat layers used in FR laminates. The laminated plates were analyzed under three different boundary conditions: simple-simple-simple-simple, free-fixed-fixed-fixed, and simple-simple-fixed-fixed. Three different plate thicknesses, t, were used: 2, 3, and 4 mm. Four different aspect ratios (a/b) were considered: 1.0, 1.2, 1.5, and 2.0. The length, a, was held constant at 0.5 m and the width, b, was varied between 0.5, 0.41666, 0.3333, and 0.25 m. The mat orientation of the $90/+\theta/-\theta$ stitched mat was varied for θ=15, 30, 45, and 60 degrees. Combinations of each of these variables were analyzed for a laminated reinforced plate consist of 12 layers using ANSYS.

The element used for the laminated plates was Shell99, which is an 8- node linear layered structural shell element (See Fig. 5). The element has six degrees of freedom at each node: translations in the x, y, and z directions and rotations about the nodal x, y, and z-axes. The Shell99 element is perfectly suited for composites materials because it allows entry of up to 250 layers. Each layer has its own thickness, material property, and orientation. For laminated FR composites, the direction of the fibers determines the layer orientation. For each layer, the layer material properties (E_1, E_2, ν_{12}, G_{12}, G_{13}, and G_{12} listed in table 1), the orientation (angle between the layer and global coordinate system, θ, as shown in the off-axis configuration of Fig. 1), and the thickness are inputted.

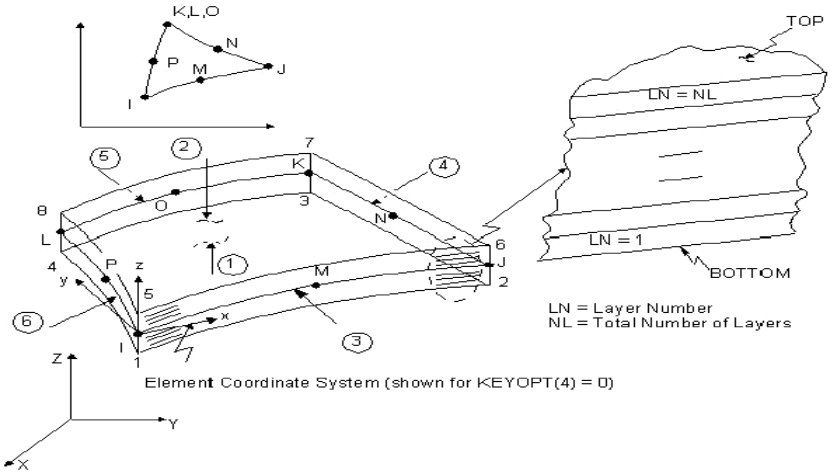

Figure 5: Shell99 Element (ANSYS Element Reference)

Table 1: Micromechanical Properties of Stiffened Layers in a Laminate E-glass/ epoxy [Barbero, 1999]

E_1 GPa	E_2 GPa	ν_{12}	$G_{12}=G_{13}$ GPa	G_{23} GPa
37.8522	6.57	0.3001	2.3924	3.0681

4. Results and Discussion

Table 2, show the critical buckling loads obtained for a laminated plate simply supported on all edges using Eq. 19 and ANSYS. The ANSYS results for simply supported laminated plates with

stacking sequence of 90/+15/-15, as expected, are less than the critical buckling load determined by using the specially orthotropic approximation (Eq. 19), with a maximum percent difference of –27.4 % and a minimum percent difference of –1.85 %. Also as expected, the 0.004 m thick plates, which had the highest values for D_{16} and D_{26}, gave the highest percent difference. As aspect ratio and thickness increases, the effect of bend twist coupling on the buckling load increases. This comparison proved the reliability of using ANSYS with high efficiency.

What wasn't expected was that most of the laminated plates with aspect ratio of 2.0 had, at its critical buckling load, a mode two buckled shape (m = 2, see Fig. 6). The laminated plates that had a mode two-buckled shape are indicated with the larger bold numbers in Table 2. At first when using Eq. 19 to predict the buckling load of the laminates, m = 1 was used in the equation, but after the ANSYS results were acquired, Eq. 19 was re-evaluated for aspect ratio of 2.0 using m = 2. After using m = 2 in Eq. 19, the equation did produce lower buckling loads for aspect ratio of 2.0.

Table 2: Laminate Plate Buckling Loads for (90/+15/-15): Simple-Simple-Simple-Simple

a (m)	b (m)	Aspect Ratio (a/b)	Plate Thickness (m)	Calculated Critical Buckling Load $(Nx)_{cr}$ (kN)	ANSYS Critical Buckling Load $(Nx)_{cr}$ (kN)	Percent Difference
0.5	0.5	1	0.002	0.823	0.808	-1.85%
0.5	0.4166	1.2	0.002	1.068	1.033	-3.4%
0.5	0.3333	1.5	0.002	1.385	1.330	-4.2%
0.5	0.25	2	0.002	**1.769**	**1.626**	-8.8%
0.5	0.5	1	0.003	2.896	2.727	-6.2%
0.5	0.4166	1.2	0.003	3.729	3.482	-7.1%
0.5	0.3333	1.5	0.003	4.864	4.483	-8.5%
0.5	0.25	2	0.003	**6.449**	**5.475**	-17.8%
0.5	0.5	1	0.004	7.094	6.438	-10.2%
0.5	0.4166	1.2	0.004	9.154	8.218	-11.4%
0.5	0.3333	1.5	0.004	12.136	10.572	-14.8%
0.5	0.25	2	0.004	**16.435**	**12.901**	-27.4%

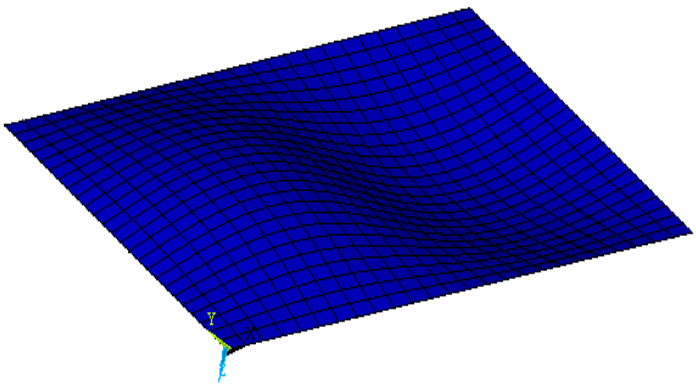

Figure 6: Mode 2 Buckled Shape, (m = 2)

The effect of mat orientation on the critical buckling load is illustrated in Fig. 7. It can be observed that for the laminated plate simply supported on all edges, the laminated plates with mats orientated at 90/+45/-45 yielded the greatest buckling load for all thicknesses with aspect ratios of 1.0 and 2.0. For an aspect ratios of 1.2 and 1.5 the laminated plates with mats orientated at 90/+30/-30 yielded the greatest buckling load for all thicknesses considered. The results for the laminated plates simply supported on all edges agree, except for an aspect ratio of 1.2 and 1.5, with the results of Pandey and Sherbourne [1991] who analytically observed that a +45/-45 orientation yielded the greatest buckling load for simply supported laminated plates under uniform compressive loading.

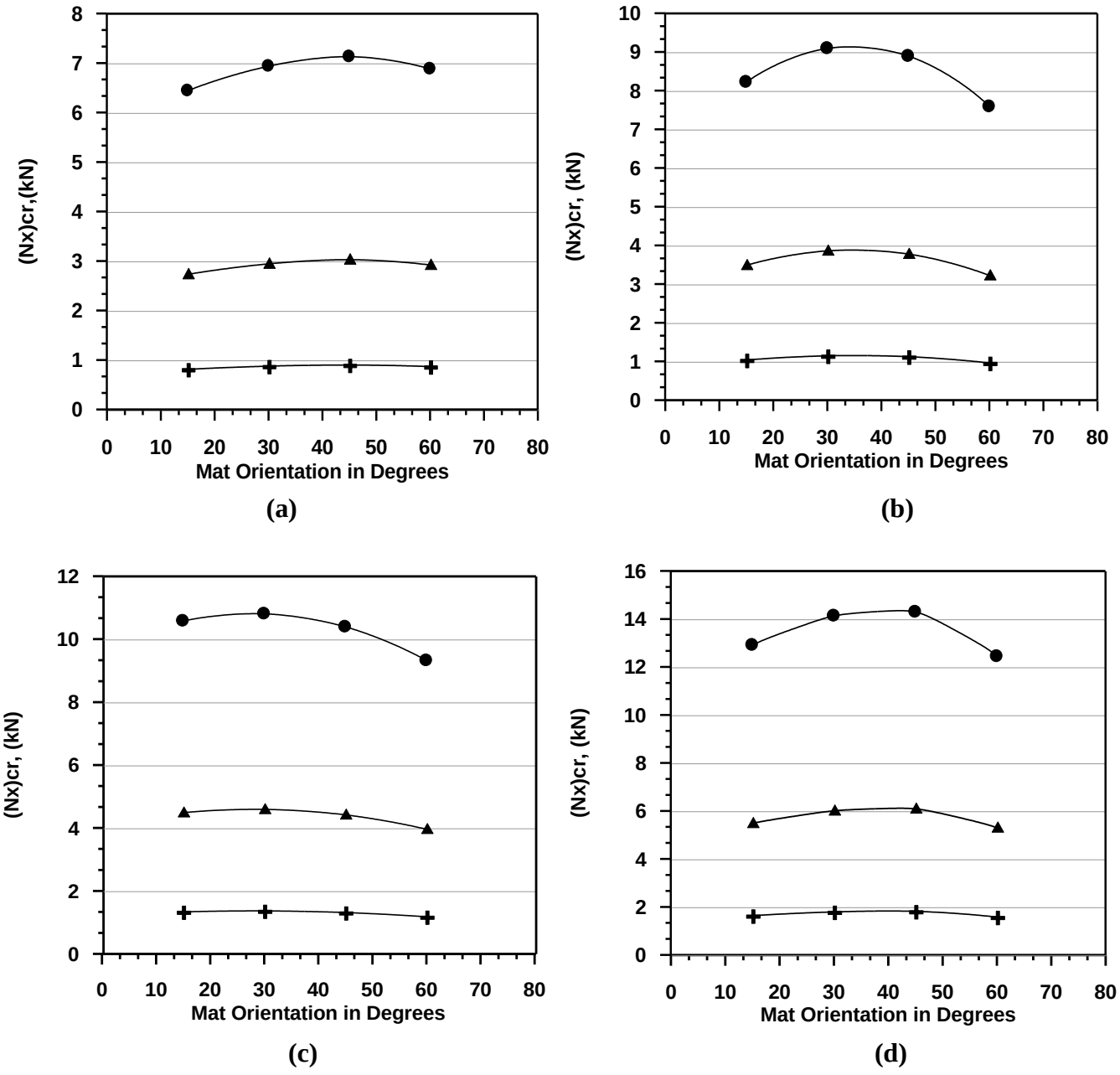

Figure 7: ANSYS Buckling Load versus Mat orientation, Simple-Simple-Simple-Simple (a) for a/b=1, (b) for a/b=1.2, (c) for a/b=1.5, and (d) for a/b=2.(+, t=0.002m, ▲,t=0.003m, ●,t=0.004m)

In the case of simple-simple-fixed-fixed shown in Fig. 8, the +30/-30 orientation produce the highest buckling load for all aspect ratios cases considered; while for free-fixed- fixed- fixed the

+15/-15 did in the majority of the cases as shown in Fig. 9. Also, it is clear that buckling load seems insensitive to changes in mat orientation when the plate thickness decrease and show almost flat curves for buckling load versus mat orientation. For all cases of the boundary conditions, critical buckling loads increase with increasing aspect ratio and of course with increasing plate thickness.

From the results, it can be conclude that each of boundary conditions, mat orientation, aspect ratio, and plate thickness have a considerable effect on the critical buckling load. Thus, it is very important to take care in the design of the laminated fiber reinforced plate subjected to in-plane compressive load.

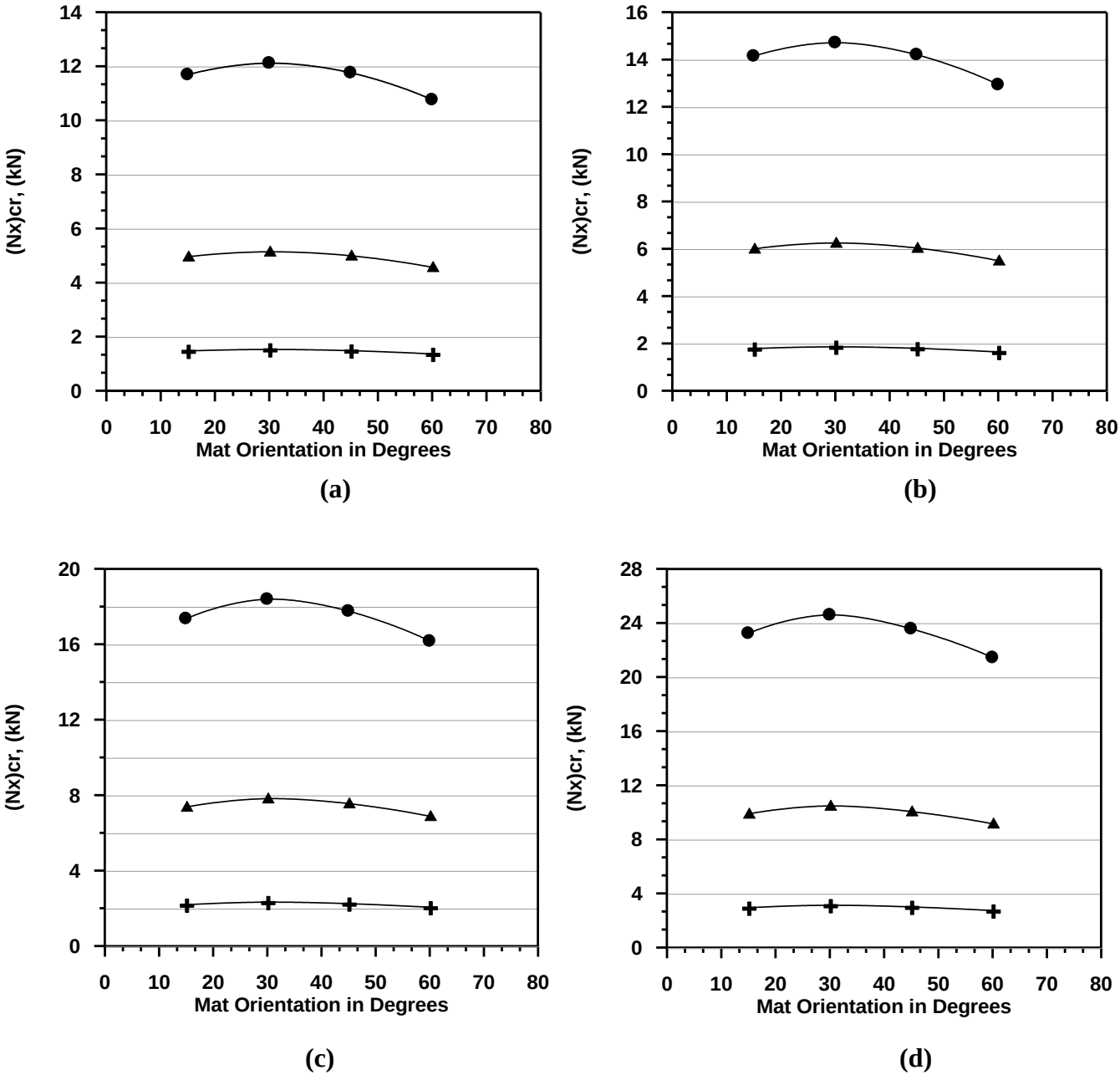

Figure 8: ANSYS Buckling Load versus Mat orientation, Simple-Simple-Fixed-Fixed (a) for a/b=1, (b) for a/b=1.2, (c) for a/b=1.5, and (d) for a/b=2.(+, t=0.002m, ▲,t=0.003m, ●,t=0.004m)

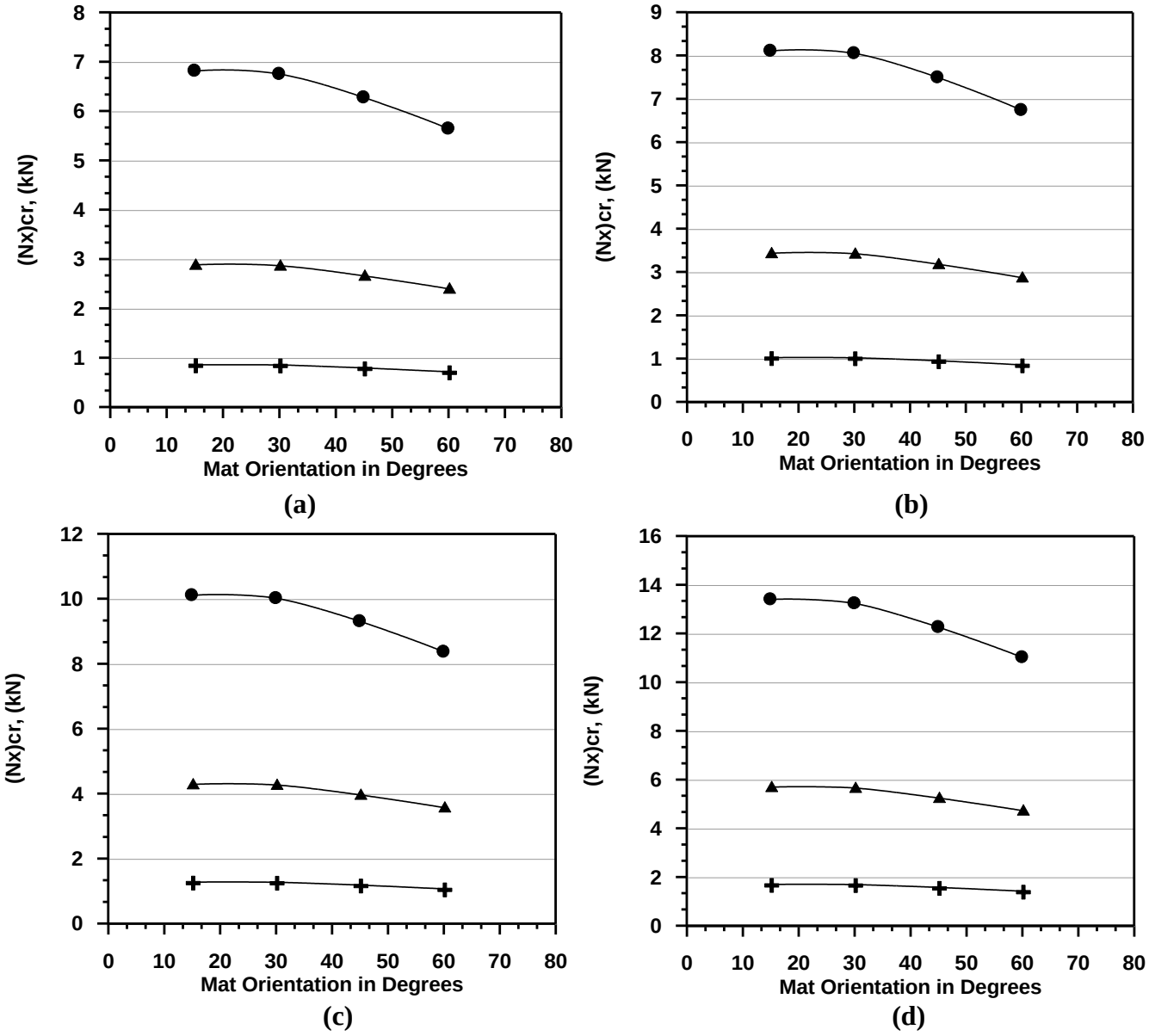

Figure 9: ANSYS Buckling Load versus Mat orientation, Free-Fixed-Fixed-Fixed (a) for a/b=1, (b) for a/b=1.2, (c) for a/b=1.5, and (d) for a/b=2.(+, t=0.002m, ▲,t=0.003m, ●,t=0.004m)

REFERENCES

Huyton, P. and York,C. B.(2001) "buckling of skew plates with continuity or rotational edge restraint", Journal Of Aerospace Engineering .

Brian, F. T. (1998)"Analysis and Design of Variable Stiffness Composite Cylinders" Ph.D. Thesis, Virginia Polytechnic Institute and State University, Blacksburg, Virginia, USA.

Barbero, E.J., (1999) *Introduction to Composite Material Design*, Taylor & Francis, Philadelphia, PA.

Timoshenko, S.P., (1961), *Theory of Elastic Stability*, McGraw-Hill, New York.

Vakiener, A.R., Zureick, A., and Will, K.M., (1991), "Prediction of Local Flange Buckling in Pultruded Shapes by Finite Element Analysis", *Advanced Composite Materials in Civil Engineering Structures*, S. L. Iyer Ed., ASCE, N. Y., pp. 303- 312.

Ashton, J.E. and Waddoups, M.E., (1969), "Analysis of Anisotropic Plates", *Journal of Composite Materials*, Vol. 3, pp. 148-165.

Ashton, J.E. and Whitney, J.M., (1970), *Theory of Laminated Plates*, Technomic, Stamford, Conn.

Bao, G., Jiang, W., and Roberts, J.C., (1997), Analytic and Finite Element Solutions for Bending and Buckling of Orthotropic Rectangular Plates", *Int. J. Solids Structures*, Vol. 34, No. 14, pp. 1797-1822.

Veres, I.A. and Kollar, L.P., (2001), "Buckling of Rectangular Orthotropic Plates Subjected to Biaxial Normal Forces", *Journal of Composite Materials*, Vol. 35, No.7, pp. 625-635.

Khdeir, A.A., (1989), "Stability of Antisymmetric Angle-Ply Laminated Plates", *Journal of Engineering Mechanics*, Vol. 115, No. 5, pp.952-963.

Pandey, M.D. and Sherbourne, A.N. (1991), "Buckling of Anisotropic Composite Plates Under Stress Gradient", *Journal of Engineering Mechanics*, Vol. 117, No. 2,pp.260-275.

Chen, W., (1994), "Buckling Mode Change of Antisymmetric Angle-Ply Laminates", *Journal of Engineering Mechanics*, Vol. 120, No. 3, pp.661-669.

Jones, R.M., (1999), *Mechanics of Composite Materials*, Taylor & Francis, Philadelphia, PA.

Staab, G.H., (1999), *Laminar Composites*, Butterworth-Heinemann, Boston, Mass.

Reddy, J.N., (1997), *Mechanics of Laminated Composite Plates*, CRC Press, Boca Raton.